Biomed Microdevices (2006) 8: 35–41
DOI 10.1007/s10544-006-6380-z

Microfluidic alignment of collagen fibers for *in vitro* cell culture

Philip Lee · Rob Lin · James Moon · Luke P. Lee

Abstract Three dimensional gels of aligned collagen fibers were patterned *in vitro* using microfluidic channels. Collagen fiber orientation plays an important role in cell signaling for many tissues *in vivo*, but alignment has been difficult to realize *in vitro.* For microfluidic collagen fiber alignment, collagen solution was allowed to polymerize inside polydimethyl siloxane (PDMS) channels ranging from 10–400 μm in width. Collagen fiber orientation increased with smaller channel width, averaging 12 ± 6 degrees from parallel for channels between 10 and 100 μm in width. In these channels 20–40% of the fibers were within 5 degrees of the channel axis. Bovine aortic endothelial cells expressing GFP-tubulin were cultured on aligned collagen substrate and found to stretch in the direction of the fibers. The use of artificially aligned collagen gels could be applied to the study of cell movement, signaling, growth, and differentiation.

Keywords Microfluidic · Collagen · Alignment · Cell culture · PDMS

Introduction

A primary goal of tissue engineering is to provide an *in vitro* microenvironment that closely resembles physiological conditions. Fine control over the chemical and spatial properties of the culture are required for successful engineering of tissues. An important aspect of the cellular environment is the presence of an extracellular matrix (ECM), which has been shown to affect growth, adhesion, differentiation, morphology, and cell signaling in multiple cell lines (Kleinman, 1987; Martin, 1981). More recent studies have revealed that the three-dimensional architecture of ECM hydrogels plays an important role in cell behavior (Cukierman, 2001; Grant, 1992; O'Shaughnessy, 2003; Stegemann, 2003). The presence of aligned collagen fibers in vascular walls acts as a signaling factor for platelet activation, which is clinically relevant for atherothrombosis (Ruggeri, 2002). The ability to manipulate the spatial organization of the ECM in cell culture is a vital for understanding *in vivo* cell behaviors.

Microfabrication provides a promising technology for patterning and manipulating the cellular microenvironment (Chiu, 2000; Jeon, 2002). Microstructured silicon and glass substrates have been shown to polarize cell morphology (Dalby, 2003; Yoshinari, 2003), bias migration (Wojciak-Stothard, 1996), and guide neurite extension (Dubey, 1999; Nagata, 1993; Rajnicek, 1997; Webb, 1995). Neurite orientation and guidance have also been investigated by micropatterning of the ECM to direct growth of nerve cells (Miller, 2001; Vogt, 2003). The development of soft lithography using polydimethyl siloxane (PDMS) enabled studies relating microfluidically patterned collagen matrices and their effect on cell growth and behavior (Chen, 1997; Liu, 2002; Tan, 2003). The integration of microfabrication with tissue engineering has enhanced control of ECM patterning to the cellular length scale. The next level of precision is to recreate *in vitro* the molecular architecture of the ECM.

Collagen type I, the major constituent of most ECM, typically exists in nature as fibers 50 nm in diameter and several microns in length. The precise spatial organization of collagen fibers *in vivo* determines properties such as the tensile strength in tendons (Pins, 1997; Tower, 2002) and the transparent tissue of the cornea (Connon, 2003; Newton, 1998). The molecular alignment of collagen is also believed to play a

P. Lee · R. Lin · J. Moon · L. P. Lee (✉)
Biomolecular Nanotechnology Center, Berkeley Sensor and Actuator Center, Department of Bioengineering, University of California, Berkeley
e-mail: lplee@berkeley.edu

role in cell signaling and development, and has been reported to orient fibroblast cells in culture (Glass-Brudzinski, 2002; Guido, 1993). The role of collagen alignment *in vivo* has also been shown to be important for directing cell proliferation and migration after injury (Matsumoto, 1998). It is therefore advantageous to engineer tissues consisting of aligned collagen matrix to exploit these physiological and mechanical advantages. However, nearly all *in vitro* preparations of ECM produce randomly oriented collagen fibrils due to the self-assembly of soluble collagen subunits (Kadler, 1996). Studies involving aligned collagen fiber substrates have relied on animal explants (Awad, 1999), magnetic alignment (Dubey, 1999; Tranquillo, 1996), and rotational seeding (Evans, 2003; Nasseri, 2003). While these methods offer the potential for more widespread cell behavior experimentation, the specialized preparation required prevents widespread application in cell biology.

In this paper, we propose a method for the microfluidic alignment of collagen fibrils *in vitro* for use in the study of cell behavior in culture. The microfluidic method allowed the molding of a 3-D matrix environment that more closely mimicked physiologic ECM while retaining the advantages of micropatterning. This technique for producing oriented collagen fibers is applicable to standard tissue culture experiments, and may prove beneficial in exploring the influence of the molecular alignment of ECM on cellular behavior. The rapid fabrication and low cost of this patterning method also make it readily adaptable to high throughput cell culturing.

Materials and methods

Microchannel fabrication

A CAD layout of the microchannels was designed with sets of channels 1 cm in length by 10, 20, 30, 40, 50, 100, 150, 200, 300, and 400 μm in width. A 4 inch chrome mask was generated and used to photolithographically pattern the channel mold. The polymer photoresist SU-8 50 (MicroChem Corp., Newton, MA) was used as the mold material. The photoresist was spin coated at 3,000 rpm for 30 seconds to create a film thickness of 40 μm on a 4 inch silicon wafer. The SU-8 was pre-baked at 65°C for 5 minutes and soft baked at 95°C for 15 minutes. The pattern was transferred by contact lithography and exposed to near UV light at 400 mJ/cm^2. A post exposure bake was conducted at 65°C for 1 minute and 95°C for 5 minutes. SU-8 Developer (MicroChem Corp., Newton, MA) was used for 6 minutes with gentle agitation to remove the non-crosslinked photoresist. A mold thickness of 100 μm was used for the 200, 300, and 400 μm width. This was created by spin coating SU-8 at 1,000 rpm, and adjusting subsequent steps according to the manufacturer. Microfluidic structures were cast from the mold with PDMS elastomer (Dow Corning, USA) as previously described (Folch, 1999). The cured polymer was removed from the mold and treated with oxygen plasma, forming hydrophilic microchannels. Each set of parallel channels was cut with a razor blade to expose the inlets and outlets and reversibly bonded to a glass coverslip.

Collagen gel preparation

Rat-tail type I collagen (BD Biosciences, Bedford, MD) solubilized in 0.02 N acetic acid was brought to physiological pH with 0.1 N NaOH and diluted with 2X Dulbecco's modified Eagle's medium (DMEM; Gibco BRL, Grand Island, NY) or 2X PBS to a final concentration of 1.5 mg/ml. Immediately after mixing ($t = 0$), collagen gel solutions were introduced into the microchannels to observe fibrillogenesis. The channels were filled using two methods: without flow and with flow. For the "no flow" condition, the collagen solution was pipetted directly on top of the PDMS microchannels and subsequently sealed with a glass coverslide. For pressure driven flow, a volume of collagen solution sufficient to immerse the inlet channels ($\sim$15 μl) was pipetted and the channels were filled at $\sim$5–10 mm/s by applying a vacuum to the opposite end of the channel. After the collagen solution had filled the volume of the channels, the external pressure was removed. For the control, collagen solution was pipetted directly onto the glass coverslide without a PDMS mold. Collagen polymerization in all experiments was conducted under static flow conditions and room temperature (25°C).

Confocal microscopy

Scanning confocal microscopy was utilized to visualize unstained collagen fibers as previously described (Brightman, 2000, Voytik-Harbin, 2001). Briefly, laser light with a wave length of 488 nm was illuminated onto the samples, and the reflected light was detected with a photomultiplier tube (PMT) using a blue reflection filter on a Leica TCS SL confocal microscopy system. A 40X oil immersion objective lens was used for all micrographs. Multiple sections 0.3–0.5 μm in thickness were captured, allowing the resolution of single collagen fibrils as well as their growth over time. For imaging of GFP tubulin transfected cells, an excitation wavelength of 488 nm was used.

Image analysis

The degree of collagen alignment within the channels was quantified with NIH ImageJ 1.3v software. A threshold value of the reflection intensity was selected to isolate collagen fibers, and their angle with the flow direction of the channel was determined by fitting each fiber to the major axis an ellipse. Depending on the width of the channel and the

microscope zoom, a given image contained between 50–700 individual collagen fibers. For each channel geometry, analysis was performed on at least 3 different replicas. Calculation of the average fiber angle was done by taking the mean of the difference of angles between each fiber and the channel axis. An angle of 0° corresponded to an orientation parallel to the channel walls. To plot the distribution of fiber angles, the data were categorized into bins of 10 degree angles ($0 \pm 5^\circ$, $10 \pm 5^\circ$, etc.) and their relative frequency was calculated.

Cell culture

Primary bovine aortic endothelial cells (BAEC) were cultured in DMEM with 10% fetal bovine serum (FBS), 1% sodium pyruvate, and 1 mM penicillin-streptomycin, all obtained from Gibco BRL (Grand Island, NY). The cells were maintained in 60 mm dishes at 37°C and 5% CO_2. BAEC cells were transfected with GFP tubulin using the lipofectamine protocol (Invitrogen, Carlsbad, CA). Cell culture on micropatterned collagen channels was performed following a previously described procedure (Thakar, 2003). Prior to collagen introduction, the PDMS channels were treated with 1% BSA for 20 minutes to prevent adhesion. The mold was placed on a LabTek chambered coverglass (NUNC, Roskilde, Denmark), filled with collagen solution, and set to polymerize at 37°C for 30 minutes. After collagen polymerization, the device was exposed to UV light for 30 minutes to crosslink the fibers and sterilize the device. The PDMS mold was then removed, and the integrity of the collagen pattern was verified via microscopy. BAEC cells were introduced at $2 \cdot 10^5$ cells/ml after being trypsinized from a confluent culture. The cells were incubated at 37°C for 1–2 hours to allow cell attachment and spreading. The chambered coverglass was then mounted onto the confocal microscope for visualization. For cell imaging, multiple z-axis scans were averaged to portray the entire depth of the 3-D collagen and cell sample.

Statistics

Analysis of quantitative data was performed using a two-tailed Student *t* test.

Results

Effect of channel width and initial flow of collagen solution on fiber alignment

The macroscopic length scale and static fluidics of conventional 3-D collagen gel preparations in cell culture produce a matrix where the molecular orientation of individual collagen fibers is largely random. We utilized two approaches to influence collagen fiber alignment: microchannel width and flow conditions. The width of the patterned channels was varied from 10 μm to 400 μm using PDMS molding. Confocal microscopy allowed the visualization of distinct collagen fibers, indicating that channel width affects fiber organization (Figure 1). The collagen fiber alignment was quantified for microchannels subjected to initial pressure driven flow and channels filled without flow (Figure 2). The control (no microchannels) had an average orientation of $41 \pm 8^\circ$ which was within experimental error of the expected 45° deviation. In microchannels 10–100 μm in width, the average alignment of fibers with initial flow was $12 \pm 6^\circ$ compared to $31 \pm 12^\circ$ for the no flow condition. With increasing channel widths, the degree of alignment decreased and was not statistically significant when compared to control above 200 μ m ($p = 0.05$). None of the "no flow" results were statistically significant ($p = 0.05$).

Fiber orientation distribution

The distribution of fiber angles from microchannels filled with initial flow was compared against channel width (Figure 3). The control measurement indicated a fairly random distribution with no preferred fiber orientation. A preference for alignment parallel with the channel walls became more pronounced as the channel width decreased. This analysis indicated that with a 10 μm channel, over 40% of the fibers were within 5° of the channel axis. As channel width increased, this peak diminished.

Polymerization kinetics

The *in vitro* polymerization of collagen fibers proceeded on a time scale similar to previously described (Newman, 1997). Confocal scanning microscopy indicated that there were no visible collagen fibers within the microchannels immediately after filling. The first fibers appeared between 10 and 20 minutes, and the bulk of fibrillogenesis was completed by 30 minutes (Figure 4). UV spectrophotometry at 405 nm was performed to verify the time dependence of collagen fibrillogenesis at the given concentration and temperature as described in previous work (Brightman, 2000). Although the optical method quantifies only the small population of collagen fibers visible in the microscope field, the rate of fiber formation was consistent with that of the bulk solution. Our observations were consistent with previous reports that collagen fibrillogenesis follows a sigmoidal time dependence characterized by an initial lag phase and rapid growth over a short interval.

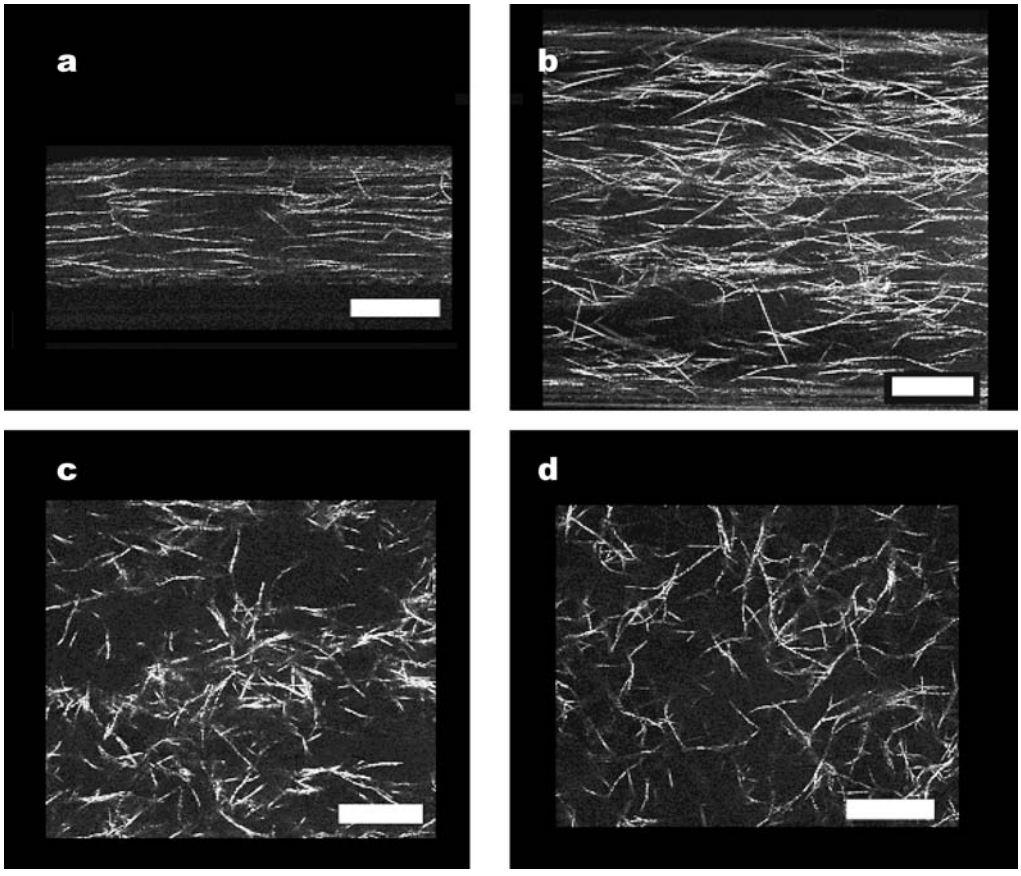

Fig. 1 Images of *in vitro* polymerized collagen fibrils in microchannels taken with reflection confocal microscopy. Channel widths were 30 μm (**a**), 100 μm (**b**), 400 μm (**c**), and without microchannel (**d**). All collagen preparations were at a final concentration of 1.5 mg/ml. Scale bar equals 20 μm in each image

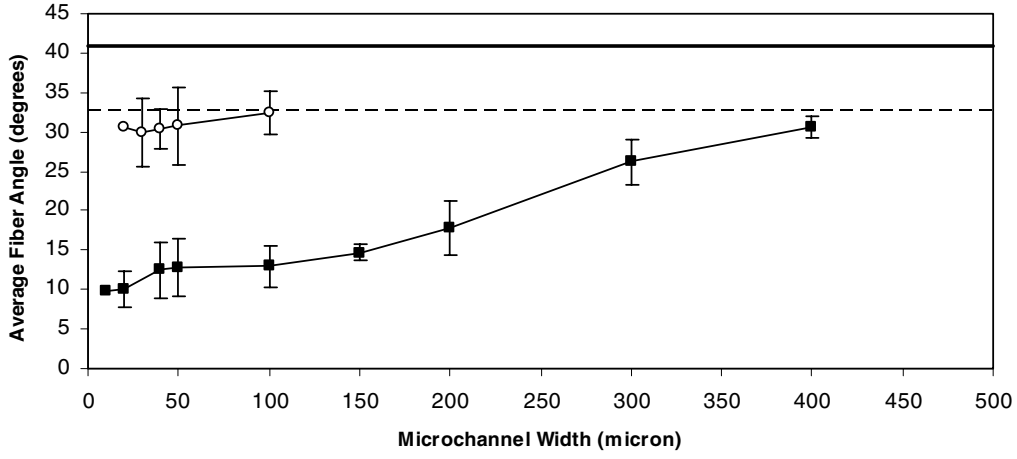

Fig. 2 Effect of microchannel width on collagen alignment. The average fiber angle was determined for collagen introduction without initial flow (○) and with initial pressure driven flow (■). The solid line indicates collagen alignment in the absence of microchannels with one standard deviation marked with the dashed line

Endothelial cell morphology

Bovine aortic endothelial cells expressing GFP tubulin were allowed to attach to the collagen patterned surface for two hours (Figure 5). Cells attached to the aligned collagen matrix were shown to spread in the direction of fiber alignment, while cells attached to the bare glass (lower left of figure) were more rounded and not preferentially aligned. Because of the 3-D nature of the cell-matrix sample (total scan depth of 22 μm), it was difficult to resolve individual microtubules.

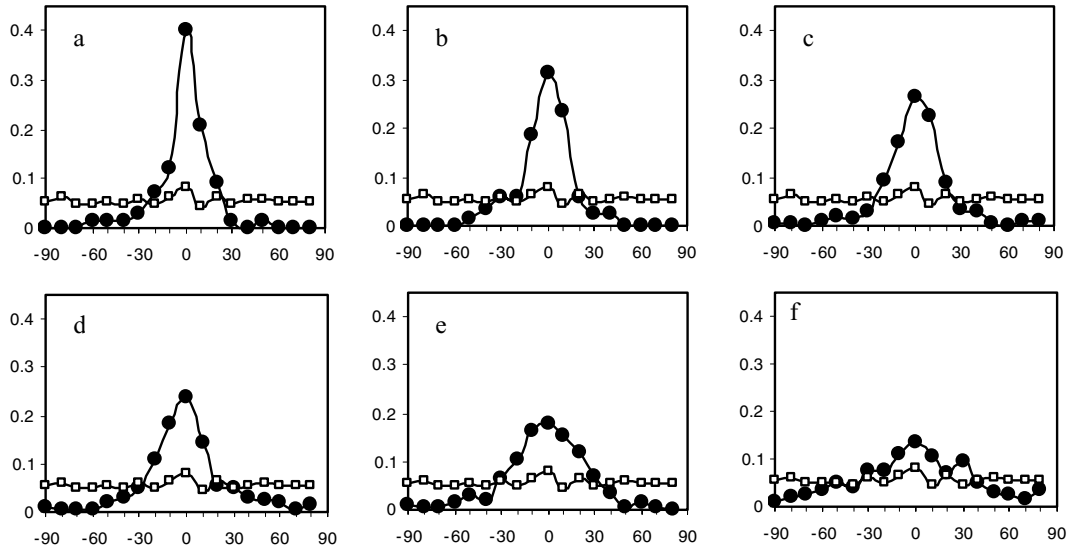

Fig. 3 Distribution of collagen fiber angles for 10 μm (**a**), 20 μm (**b**), 40 μm (**c**), 100 μm (**d**), 150 μm (**e**), and 200 μm (**f**) channel widths compared against no microchannel control (□). These histograms show the relative frequency (y-axis) of fiber angles in 10° bins (x-axis), with 0° set as parallel to the channel axis. Axes and scales are identical in (a–f).

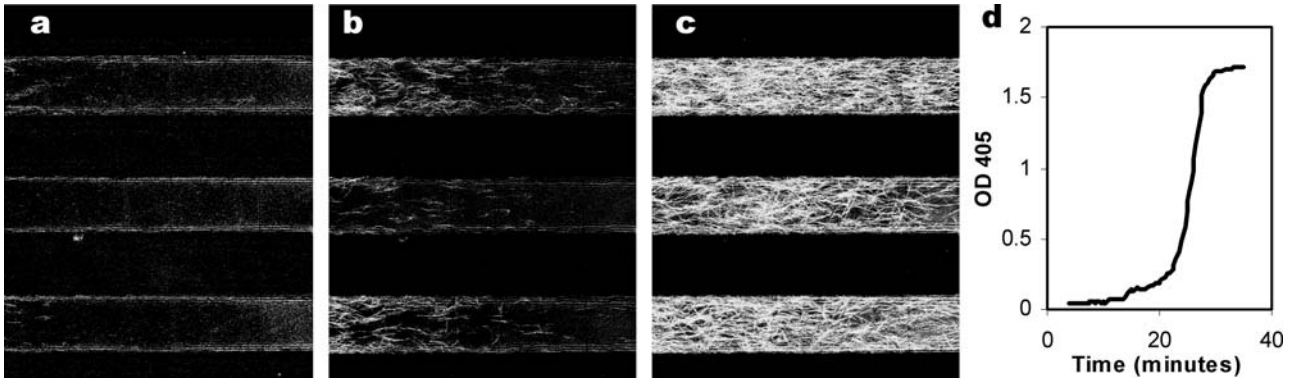

Fig. 4 Time series of collagen polymerization inside microchannels. Confocal microscopy of collagen fibers in three parallel 30 μm channels taken 19 minutes (**a**), 22 minutes (**b**), and 28 minutes (**c**) after initiation of polymerization conditions. Spectrophotometry at 405 nm of 1 ml bulk collagen solution at the same conditions indicated a similar time course (**d**).

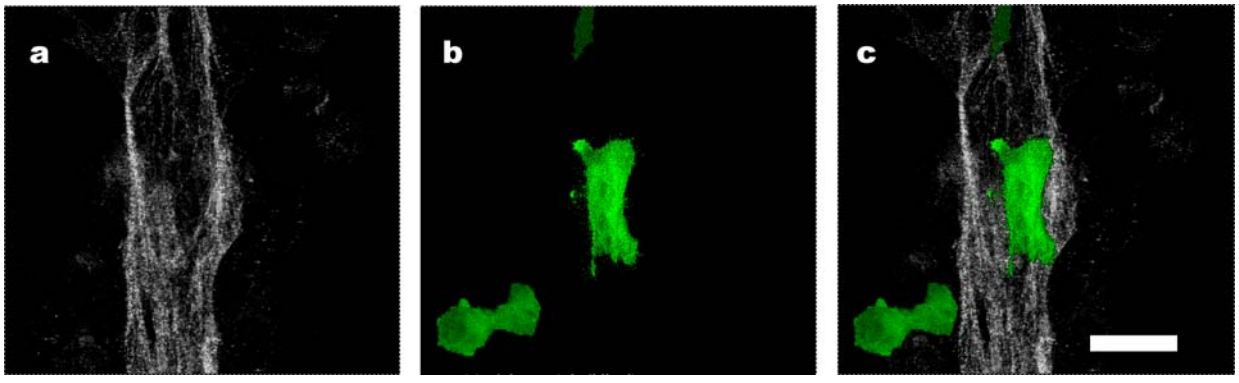

Fig. 5 Aligned collagen matrix influenced cell morphology. Bovine aortic endothelial cells were transfected with GFP tubulin and cultured on aligned collagen substrate for 2 hours at 37°C. Confocal microscopy using reflection at 488 nm resolved collagen fibers **(a)** and GFP fluorescence imaged transfected cells **(b)**. An overlay of these two images is presented in **(c)**. The scale bar represents 20 μm.

Discussion

By using widely available microfabrication technology, we were able to generate an aligned ECM substrate relevant to cell culture. This work describes the artificial alignment of three-dimensional matrices of collagen in microfluidic channels. Polymerizing collagen fibers were observed to orient parallel to the channel axis as a function of channel size. In microchannels with widths 100 μm and lower, the average fiber orientation was within 15° of parallel. As channel size increased, the degree of alignment diminished. When bovine aortic endothelial cells were cultured on the aligned matrix, there was evidence of preferential alignment along the fiber orientation direction. These results demonstrated the capability of influencing cell behavior through the molecular configuration of the ECM.

While it was apparent that collagen orientation within microchannels depended on width and the presence of initial flow, the mechanism of alignment was unclear. Two likely contributing effects were orientation by flow and geometric restriction by the channel walls. In the case of flow orientation, the effect must have been induced before collagen polymerization was visible, since the initial flow lasted only a few seconds. A possible hypothesis is that the laminar velocity profile within the channel induced the collagen "seeding" units to align at the edges of the microfluidic channels. If the fiber precursor was assumed to be cylindrical or elongated in nature, it is reasonable that a flow field would result in parallel alignment. If these nucleation sites remained immobile, subsequent fiber polymerization would occur in an aligned manner. This was supported by the observation that even at low fiber density, the smallest fibers visible with confocal microscopy appeared to be fixed in space and polymerized without significant bending. If alignment varied as a function of flow rate, then it would be predicted that fibers in the center of a channel would be more aligned than near the walls due to a parabolic flow profile. In fact, we found no relationship between position and fiber alignment for samples with flow; and in all cases studied, alignment at the center of the channel was statistically indistinguishable from the channel wall. The geometric effects of the channel walls in promoting parallel alignment appeared to play a lesser role. While fibers growing into the walls were found to be redirected, this only affected the fraction of fibers within $\sim$5 μm of the channel wall. From the "no flow" condition, this effect appeared to produce a maximum of $\sim$10° of alignment relative to control. This improvement may have been partially due to the brief movement of fluid along the channels when the glass slide was mounted on the channels. As shown in Figure 2, the presence of the channel walls alone did not result in statistically significant fiber alignment, while the addition of flow improved alignment to $\sim$15° of parallel in channels smaller than 100 μm.

As the channel size was increased, there was a gradual loss in fiber alignment. The effect of geometric constraint by the channel wall was expected to decrease with larger channels. Since collagen fibers rarely extended beyond 10 μm, very few collagen fibers will encountered the walls of large channels. The effect of increasing channel width on flow alignment was less apparent. In the larger channels, the alignment of collagen fibers appeared to be less uniform. This trend was evident when the images in Figure 1 were compared. Currently, the flow alignment of collagen fibers appears to only work at the microscale. When the channel width was extended to 400 μm, the alignment effects became negligible. One possibility could be that the vicinity of the channel walls was vital for creating collagen nucleation sites. If the fiber precursors rapidly attached to the channel walls from solution and were able to influence additional nucleation sites within a few microns, then having larger channel dimensions would reduce fiber alignment. From Figure 4, it appeared that the existence of previously polymerized collagen fibers increased the rate of new fiber growth. These possible mechanisms are difficult to test experimentally since the kinetics of single molecule collagen polymerization in a complex environment is unknown. While optimizing geometry and flow conditions in the microchannels need to be further explored, the conditions used in this experiment were capable of producing an aligned ECM matrix on a scale suitable for the study of cellular behavior.

The alignment of extracellular matrix fibers plays an important role in patterning cells within tissues. Bovine aortic endothelial cells (BAEC) were cultured to observe changes in cell morphology in response to aligned collagen substrate. This cell type has previously been used to study interactions with the culture substrate due to their physiologic sensitivity to ECM conditions (Kuzuya, 1999; Thakar, 2003; Thoumine, 1995). Adhesion of an endothelial cell to the substrate determines how the cell spreads and migrates. Figure 5 suggests that an aligned collagen substrate influenced BAEC endothelial cells and promoted directional elongation. Aligned collagen fibers presumably had an effect on the formation of cell contacts such as focal adhesions, which play a role in cytoskeletal reorganization (Kaverina, 2002). While the biology of how an aligned collagen substrate affects cell behavior was not investigated in this work, our observations support the belief that an aligned matrix is important for many cellular functions. Further research in the role of aligned ECM in cell signaling, migration, and differentiation may yield useful results for tissue engineering.

Much recent work has focused on the ability of microfabrication technology to aid in replicating the *in vivo* tissue environment (Griffith, 2002). The ability to align collagen fibers within microscale devices offers an additional degree of control for *in vitro* cell culture, and may prove useful for the patterning of cells and tissues. An exciting possibility

exists for using microfluidic devices for neural engineering. If neurons could be manipulated with an aligned collagen matrix, this could be used to provide a more natural substrate environment for promoting neurite growth or axon path finding (O'Connor, 2001). It should also be possible to implement directed chemical stimulation of cultured cells grown on patterned ECM to observe phenotypic response (Miller, 2002). The combination of these techniques is well suited for the development of high throughput cell culture assays. The advance of microfluidic devices into the field of tissue engineering could benefit from the ability to produce aligned collagen matrices.

Acknowledgments

Microchannel fabrication was performed in the University of California, Berkeley Microlab. We would like to thank Ki-hun Jeong and Paul Hung for providing support in microfabrication and Julia Chu for assisting in cell culture.

References

H.A. Awad, D.L. Butler, G.P. Boivin, F.N. Smith, P. Malaviya, B. Huibregtse, and A.I. Caplan, Tissue Eng **5**, 267–277 (1999).
A.O. Brightman, B.P. Rajwa, J.E. Sturgis, M.E. McCallister, J.P. Robinson, and S.L. Voytik-Harbin, Biopolymers **54**, 222–234 (2000).
C.S. Chen, M. Mrksich, S. Huang, G.M. Whitesides, and D.E. Ingber, Science **276**, 1425–1428 (1997).
D.T. Chiu, N.L. Jeon, S. Huang, R.S. Kane, C.J. Wargo, I.S. Choi, D.E. Ingber, and G.M. Whitesides, Proc Natl Acad Sci USA **97**, 2408–2413 (2000).
C.J. Connon and K.M. Meek, Wound Repair Regen **11**, 71–78 (2003).
E. Cukierman, R. Pankov, D.R. Stevens, and K.M. Yamada, Science **294**, 1708–1712 (2001).
M.J. Dalby, M.O. Riehle, S.J. Yarwood, C.D. Wilkinson, and A.S. Curtis, Exp Cell Res **284**, 274–282 (2003).
N. Dubey, P.C. Letourneau, and R.T. Tranquillo, Exp Neurol **158**, 338–350 (1999).
H.J. Evans, J.K. Sweet, R.L. Price, M. Yost, and R.L. Goodwin, Am J Physiol Heart Circ Physiol **285**, H570–578 (2003).
A. Folch, A. Ayon, O. Hurtado, M.A. Schmidt, and M. Toner, J Biomech Eng **121**, 28–34 (1999).
J. Glass-Brudzinski, D. Perizzolo, and D.M. Brunette, J Biomed Mater Res **61**, 608–618 (2002).
D. Grant, M. Cid, M.C. Kibbey, and H. Kleinman, Lab Invest **67**, 805-806; author reply 807–808 (1992).
L.G. Griffith, Ann N Y Acad Sci **961**, 83–95 (2002).
S. Guido and R.T. Tranquillo, J Cell Sci **105 (Pt 2)**, 317–331 (1993).
K.E. Kadler, D.F. Holmes, J.A. Trotter, and J.A. Chapman, Biochem J **316**(Pt 1), 1–11 (1996).
I. Kaverina, O. Krylyshkina, and J.V. Small, Int J Biochem Cell Biol **34**, 746–761 (2002).
H.K. Kleinman, L. Luckenbill-Edds, F.W. Cannon, and G.C. Sephel, Anal Biochem **166**, 1–13 (1987).
M. Kuzuya, S. Satake, M.A. Ramos, S. Kanda, T. Koike, K. Yoshino, S. Ikeda, and A. Iguchi, Exp Cell Res **248**, 498–508 (1999).
N.L. Jeon, H. Baskaran, S.K. Dertinger, G.M. Whitesides, L. Van de Water, and M. Toner, Nat Biotechnol **20**, 826–830 (2002).
V.A. Liu, W.E. Jastromb, and S.N. Bhatia, J Biomed Mater Res **60**, 126–134 (2002).
G.R. Martin and H.K. Kleinman, Hepatology **1**, 264–266 (1981).
N. Matsumoto, S. Horibe, N. Nakamura, T. Senda, K. Shino, and T. Ochi, Arch Orthop Trauma Surg **117**, 215–221 (1998).
C. Miller, S. Jeftinija, and S. Mallapragada, Tissue Eng **7**, 705–715 (2001).
C. Miller, S. Jeftinija, and S. Mallapragada, Tissue Eng **8**, 367–378 (2002).
I. Nagata, A. Kawana, and N. Nakatsuji, Development **117**, 401–408 (1993).
B.A. Nasseri, I. Pomerantseva, M.R. Kaazempur-Mofrad, F.W. Sutherland, T. Perry, E. Ochoa, C.A. Thompson, J.E. Mayer, Jr., S.N. Oesterle, and J.P. Vacanti, Tissue Eng **9**, 291–299 (2003).
S. Newman, M. Cloitre, C. Allain, G. Forgacs, and D. Beysens, Biopolymers **41**, 337–347 (1997).
R.H. Newton and K.M. Meek, Biophys J **75**, 2508–2512 (1998).
S.M. O'Connor, D.A. Stenger, K.M. Shaffer, and W. Ma, Neurosci Lett **304**, 189–193 (2001).
T.J. O'Shaughnessy, H.J. Lin, and W. Ma, Neurosci Lett **340**, 169–172 (2003).
G.D. Pins, D.L. Christiansen, R. Patel, and F.H. Silver, Biophys J **73**, 2164–2172 (1997).
A. Rajnicek, S. Britland, and C. McCaig, J Cell Sci **110**(Pt 23), 2905–2913 (1997).
Z.M. Ruggeri, Nat Med **8**, 1227–1234 (2002).
J.P. Stegemann and R.M. Nerem, Exp Cell Res **283**, 146–155 (2003).
W. Tan and T.A. Desai, Tissue Eng **9**, 255–267 (2003).
R.G. Thakar, F. Ho, N.F. Huang, D. Liepmann, and S. Li, Biochem Biophys Res Commun **307**, 883–890 (2003).
O. Thoumine, R.M. Nerem, and P.R. Girard, Lab Invest **73**, 565–576 (1995).
T.T. Tower, M.R. Neidert, and R.T. Tranquillo, Ann Biomed Eng **30**, 1221–1233 (2002).
R.T. Tranquillo, T.S. Girton, B.A. Bromberek, T.G. Triebes, and D.L. Mooradian, Biomaterials **17**, 349–357 (1996).
A.K. Vogt, L. Lauer, W. Knoll, and A. Offenhausser, Biotechnol Prog **19**, 1562–1568 (2003).
S.L. Voytik-Harbin, B. Rajwa, and J.P. Robinson, Methods Cell Biol **63**, 583–597 (2001).
A. Webb, P. Clark, J. Skepper, A. Compston, and A. Wood, J Cell Sci **108 (Pt 8)**, 2747–2760 (1995).
B. Wojciak-Stothard, A. Curtis, W. Monaghan, K. MacDonald, and C. Wilkinson, Exp Cell Res **223**, 426–435 (1996).
M. Yoshinari, K. Matsuzaka, T. Inoue, Y. Oda, and M. Shimono, J Biomed Mater Res A **65**, 359–368 (2003).